a C_s geometry (neglecting the presence of the cation). Spectra of the $SO_2F_3^-$ anion were similar to those of known 40-electron species, including the chlorine counterpart, ClO_2F_3, and suggested a trigonal-bipyramidal structure with the two oxygen atoms in equatorial positions.

It is interesting also to note trends in reactivity in the current study. Samples of SOF_2 contained some impurity SO_2 in all experiments, and the yield (based on band intensities) of the SO_2 reaction product with CsF was greater than the yield of reaction product of CsF with SOF_2. One might infer a considerably greater cross section for the reaction of CsF with SO_2 relative to SOF_2. Likewise, while normal samples of SO_2F_2 did not contain any SO_2, samples of $S^{18}O_2F_2$ did contain some labeled SO_2 as well. Here, too, the yield of SO_2F^- was relatively greater than the yield of $SO_2F_3^-$, again indicating a greater reaction cross section with SO_2 than with SO_2F_2. While no attempt was made to compare relative reactivities of SOF_2 and SO_2F_2, product yields seem to indicate that SO_2F_2 is more reactive toward CsF than is SOF_2.

Acknowledgment. The authors gratefully acknowledge support of this research by the National Science Foundation, through grant CHE8100119, and B.S.A. thanks the Dreyfus Foundation for a Teacher-Scholar Grant. Dr. F. T. Prochaska is also gratefully acknowledged for his gift of a cylinder of SO_2F_2.

Registry No. SO_2F^-, 22539-11-3; SOF_3^-, 86527-07-3; $SO_2F_3^-$, 67269-52-7; CsF, 13400-13-0; SO_2, 7446-09-5; SOF_2, 7783-42-8.

Contribution from the DGR-SEP-SCPR, Centre d'Etudes Nucléaires de Fontenay-aux-Roses, Fontenay-aux-Roses 92260, France, and DPC-SCM, Centre d'Etudes Nucléaires de Saclay, Gif/Yvette Cedex 91191, France

Azide Interaction with 4f and 5f Ions in Aqueous Solutions. 1. Trivalent Ions

C. MUSIKAS,*† C. CUILLERDIER,† J. LIVET,† A. FORCHIONI,‡ and C. CHACHATY‡

Received November 16, 1982

Solvent extraction and UV, Raman, and NMR spectroscopic studies were carried out on trivalent actinide and lanthanide aqueous azido complexes. Unlike trivalent d transition ions ($\beta_{11} \simeq 10^5$) 5f and 4f aqueous azido complexes are weak ($\beta_{11} \simeq 2.5$ for $Nd(N_3)^{2+}$), but the trivalent actinides exhibit formation constants 1 order of magnitude higher than the lanthanides. All the spectroscopic methods indicate that we are dealing with inner-sphere complexes and actinide–lanthanide differences must be attributed to higher covalent contributions in the 5f azides. ^{15}N NMR combined with ^1H NMR served to investigate the azide binding properties. With the trivalent 5f and 4f ions the binding occurs by one of the terminal nitrogen atoms. The M–N bond distance is close to 2.75 Å. The lanthanide(III)–(linear azide) moieties are bent with a bond angle close to 135°, unlike the homologous linear thiocyanate complexes.

Introduction

The 5f- and 4f-block ions form complexes with pure nitrogen donors that are difficult to observe in aqueous solutions due to unfavorable competition with the water molecules. However, investigations dealing with 4f and 5f trivalent ion–nitrogen donor complexes are of great interest because they offer an insight into the similarities and differences in the chemical behavior of the two f series.

Moreover actinide–lanthanide group separations[1,2] have been performed from media in which the trivalent ions are engaged in complexes with ligands possessing donor atoms less electronegative than oxygen. Consequently, investigations like the one reported here could lead to new actinide–lanthanide group separation processes. In a previous paper,[3] we showed that ^{14}N, ^{15}N, and ^{13}C nuclear magnetic resonance, Raman, and UV spectroscopic measurements indicate that lanthanide thiocyanato complexes are mostly inner sphere, and consequently 4f–5f group separations from thiocyanate media stem from differences in complex stability and not from differences in complex type[4] (inner sphere for 5 f ions vs. outer sphere for 4f). The greater stabilities of the actinide complexes could be attributed to higher covalent interactions, since the ionic radii of the 4f and 5f trivalent ions are closely comparable (1.1 to 0.9 Å). This paper deals with the binding properties of azide ions with f-series trivalent ions. The d-block ions form stable complexes in aqueous solutions.[5] Raman and infrared spectroscopic results indicate[6] that in $Co(N_3)_4^{2-}$, $Zn(N_3)_4^{2-}$, and $Sn(N_3)_6^{2-}$ the M—N=N=N moieties are bent.

The crystal structures of NaN_3[7] and $Co(NH_3)_5N_3(N_3)_2$[8] have been determined, and two kinds of N_3^- ions have been identified. Ionically bonded N_3^- ions in NaN_3 and the outer-sphere N_3^- ions in $Co(NH_3)_5N_3(N_3)_2$ are linear and symmetrical with N–N distances close to 1.15 Å. In covalently bonded azide, two N=N distances are observed, the longer between central nitrogen (N_2) and bonded nitrogen (N_1). In HN_3[9] and CH_3N_3,[10] for instance, the N_1–N_2 and N_2–N_3 distances differ by 0.11 Å (1.24 against 1.13 Å, slightly more than the distances observed for the inner-sphere N_3^- of $Co(NH_3)_5N_3(N_3)_2$, i.e. 1.2 and 1.15 Å. Covalently linked moieties M—N=N=N are bent with M–N_3 bond angles as follows: 112° in HN_3, 120° in CH_3N_3, and 125° in $Co(NH_3)_5N_3(N_3)_2$.

Few reports concerning the f-block azide complexes are to be found in the literature. It has been claimed that UO_2^{2+} ions form the aqueous species $UO_2(N_3)^+ \cdot xH_2O$, $UO_2(N_3)_2 \cdot yH_2O$, and $UO_2(N_3)_3^- \cdot zH_2O$.[11] Complexes with trivalent

† Centre d'Etudes Nucléaires de Fontenay-aux-Roses.
‡ Centre d'Etudes Nucléaires de Saclay.

(1) R. E. Leuze and M. H. Lloyd, *Process Chem.*, **4**, 197 (1970).
(2) P. T. Gerontopoulos, L. Rigali, and P. G. Barbano, *Radiochim. Acta*, **4**, 75 (1965). W. W. Schulz, "The Chemistry of Americium", 1976, TID 26271-236.
(3) C. Musikas, C. Cuillerdier, and C. Chachaty, *Inorg. Chem.* **17**, 3610 (1978).
(4) P. K. Khopkar and J. N. Mathur, *J. Inorg. Nucl. Chem.*, **36**, 3819 (1974).
(5) L. G. Sillén and A. E. Martell, "Stability Constants of Metal Ion Complexes", Chemical Society, London, 1964; supplement, 1971.
(6) D. Forster and W. D. Horrocks, Jr., *Inorg. Chem.*, **5**, 1510 (1966).
(7) G. J. King, B. S. Miller, F. F. Carlson, and R. C. MacMillan, *J. Chem. Phys.*, **35**, 1442 (1961).
(8) G. J. Palenik, *Acta Crystallogr.*, **17**, 360 (1964).
(9) E. Amble and B. P. Dailey, *J. Chem. Phys.*, **18**, 1422 (1950).
(10) R. L. Livingston and C. N. R. Rao, *J. Phys. Chem.*, **64**, 756 (1960).

0020-1669/83/1322-2513$01.50/0

lanthanide ions have been reported,[12,13] and one of us investigated the NpO_2^+ aqueous azido species.[14] It was found that in concentrated sodium azide the predominant species contain four and five N_3^- ions ($NpO_2(N_3)_4^{3-}$ and $NpO_2(N_3)_5^{4-}$).

Results from 4f and 5f trivalent ion solvent extraction and spectroscopy will be discussed in this paper. Data from the former technique led mainly to the knowledge of the equilibria involved. NMR, UV–visible, and Raman spectroscopies were useful to gain an insight into azido complex geometry.

Experimental Section

Reagents. All the usual chemical reagents were analytical grade and were used without further purification, except thenoyltrifluoroacetone (TTA):

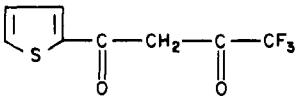

This Merck reagent, employed in extraction studies, was sublimed under vacuum before use.

^{152}Eu, ^{147}Nd, and ^{169}Yb used as tracers were provided by ISOTEC (Versailles, France), and ^{241}Am was supplied by STU (Fontenay-Aux-Roses, France).

Procedures and Apparatus. Solvent Extraction. TTA was dissolved in benzene. Organic and aqueous phases were mixed with use of a mechanical agitator immersed in a controlled-temperature water bath. We considered that the rather slow distribution equilibria were reached after 12 h of mixing.

The pH and the azide concentrations were measured after phase separation because of possible ligand losses during extraction.

Metallic species distribution coefficients were measured by quantitative γ-ray spectroscopy. The presence of several metals in the same test tube was necessary to obtain reliable separation coefficients.

γ-ray Spectroscopy. γ activities of the solvent-extraction aqueous and organic samples were counted with an ultrapure Ge detector associated with a 4000-channel Interzoom Sein analyzer. ^{241}Am (59.6 keV), ^{152}Eu, ^{153}Eu, ^{154}Eu (122 and 344 keV), ^{147}Nd (91 and 531 keV), and ^{169}Yb (63, 177, and 198 keV) were used as tracers.

NMR Spectroscopy. The ^{15}N and ^{14}N nuclear magnetic resonance analyses were performed with D_2O solutions of lanthanide perchlorate at controlled pH. As in solvent extraction, the N_3^- concentrations were measured on each sample after recording its spectrum.

A WH 90 Bruker spectrometer was used at the frequencies 6.5 MHz for ^{14}N, 9.12 MHz for ^{15}N, and 90 MHz for ^1H NMR. Subsidiary ^1H NMR measurements were performed with a 250-MHz Cameca spectrometer.

UV and Raman Spectroscopies. The UV–visible absorption measurements were performed with a Beckman 5270 or a Cary 17 double-monochromator spectrophotometer. Raman spectroscopy was carried out with a Coderg LRT 800 spectrophotometer. The light source was a Spectra-Physics 1-W krypton laser. In most cases we used the red 647.1-nm laser main line.

Solvent Extraction

The extraction of metallic chelates $M(TTA)_n$ by inert organic solvents with low dielectric constant has been used extensively for aqueous complex investgations.[15,16] For trivalent ion M^{3+}, extraction occurs according to mechanism 1; species present in organic phases are set off by vertical bars.

$$M^{3+} + 3|HTTA| \rightleftharpoons |M(TTA)_3| + 3H^+ \quad (1)$$

The presence of organic insoluble complexing ligands in the aqueous phases causes variations in the distribution coefficients,

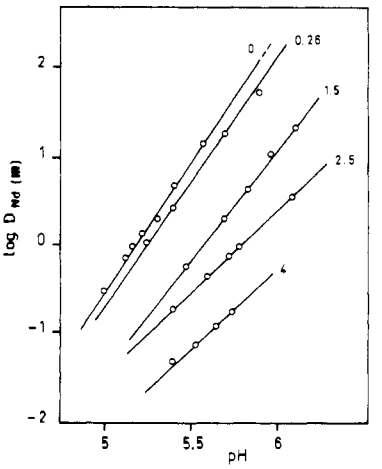

Figure 1. Distribution of Nd(III) between 0.0075 M HTTA in benzene and aqueous NaN_3 solutions as a function of pH. The figures indicate the total azide concentration (M).

Table I. Formation Constants of Trivalent 4f and 5f Ion Aqueous Azido Complexes, As Found from Extraction Data

ion	β_{11}	β_{21}	β_{31}
Nd(III)[a]	2.5	4.0	5.0
Eu(III)[b]	2.5	4.0	5.0
Yb(III)[c]	2.5	5.0	7.0
Am(III)[d]	18	40	26

[a] Obtained from a complete data set. In *Rapp. CEA-R-Fr., Comm. Energ. At., CEA-R 5140* (1981) C.C. calculated $\beta_{11} = 2$, $\beta_{21} = 8$. Here we report results of new calculations based on the same data but carried out using a model with three complexes. This model was chosen because $\delta D_{Am(III)}/\delta C_{N_3^-}$ values indicated the contribution of complexes containing more than two N_3^- ions. [b] Assigned value from the low variation of β_n as a function of Z in the 4f series. [c] Obtained from a curve of $D_{Yb(III)}/D_{Nd(III)}$ as a function of $[N_3^-]$. [d] Obtained from $D_{Eu(III)}/D_{Am(III)}$ as a function of $[N_3^-]$.

which can be expressed as a function of the complex formation constants:

$$D_{M(III)} = [|M(TTA)_3|]/[M^{3+}](1 + \beta_1 L + \beta_2 L^2 + \ldots + \beta_n L^n) \quad (2)$$

If pH and |TTA| concentrations are kept constant, eq 2 can be rewritten as

$$D_{M(III)} = D_{M(III)}^0 / \sum_{i=0}^{i=n} \beta_i L^i \quad (3)$$

In eq 2 and 3 $D_{M(III)}$ and $D_{M(III)}^0$ refer to the trivalent metal distribution coefficients, in the presence and absence of complexing agent, respectively, β_1, ..., β_n are the formation constants of the monomeric complexes containing 1, ..., n molecules of ligand, and L is the ligand concentration.

For pH values far below that of the pK_a, L concentrations were calculated from the total azide concentrations (L_t), the pH values, and the HN_3 pK_a, which was found to be 5.27 at ionic strength $\mu = 5$ (eq 4).

$$L = L_t K_a / [H^+] + K_a \quad (4)$$

For pH near that of the pK_a we preferred to calculate the N_3^- concentrations from L_t and HN_3 titrations using standard argentimetric and acidimetric methods. Several trivalent 4f distribution coefficients were measured as a function of L_t and pH. Typical Nd(III) extraction curves, at constant pH, are shown in Figure 1. The formation constants were calculated by the least-squares method using eq 3. Results for Nd(III), Eu(III), Yb(III), and Am(III) are given in Table I. A maximum of three formation constants was reliably calculated,

(11) F. G. Sherif and M. A. Awad, *J. Inorg. Nucl. Chem.*, **19**, 94 (1961).
(12) G. Vicentini and F. A. Araujo, *An. Acad. Bras. Cienc.*, **49** (4), 541 (1977).
(13) M. S. El Ezaby and I. E. Abdel Aziz, *J. Inorg. Nucl. Chem.*, **37**, 2016 (1975).
(14) C. Musikas and M. Marteau, *Sov. Radiochem. (Engl. Transl.)*, **20**, 253 (1978).
(15) R. E. Connick and W. H. MacVey, *J. Am. Chem. Soc.*, **71**, 3182 (1949).
(16) R. Guillaumont, *CNRS Res.*, **No. 154**, 165 (1966).

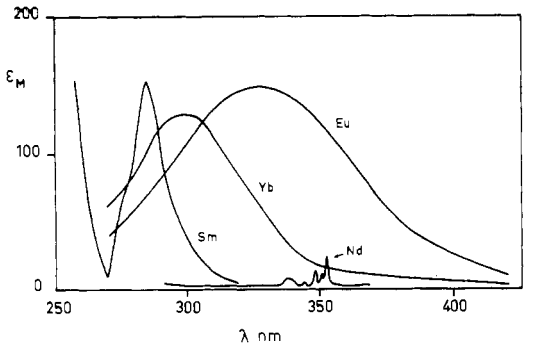

Figure 2. UV absorption spectra of Eu(III), Yb(III), Sm(III), and Nd(III) in 1.2 M sodium azide (pH 5.4, μ = 5).

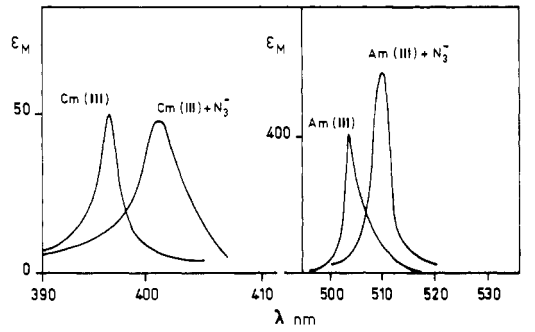

Figure 3. Effect of azide on the main Cm(III) and Am(III) f–f absorption band.

but the high slopes of the curves of $D_{Nd^{3+}}$ as a function of free N_3^- concentration suggested that complexes with more than three N_3^- groups were obtained in concentrated sodium azide solutions.

UV and Raman Spectroscopies

UV and Raman spectroscopy investigations were carried out with two objectives: to remeasure the complex formation constants and to gather structural information about the azide complexes (inner- vs. outer-sphere complexes).

The UV part of Eu^{3+}, Yb^{3+}, Sm^{3+}, and Nd^{3+} absorption spectra are shown in Figure 2. It can be seen that the spectra of the three first ions possess broad absorption bands in the range 250–350 nm. The energy of the maximum absorption decreases in the order Sm(III) > Yb(III) > Eu(III), which is the reverse order of the divalent ion stability, in agreement with the semiempirical correlations between trivalent 4f and 5f complex charge-transfer band energies and M^{3+}/M^{2+} oxidation potentials established by Nugent et al.[17]

In a review paper,[18] Jørgensen discussed thiocyanato and azido d transition ion complex charge-transfer spectra. He came to the conclusion that N-bonded thiocyanate has an optical electronegativity of 2.6 against 2.8 for azide. From the absorption maxima observed for $Eu(NCS)^{2+}$ (34.5×10^3 cm^{-1})[3] and $Eu(N_3)^{2+}$ (30.3×10^3 cm^{-1}) one can calculate

$$\chi_{opt}(NCS^-) - \chi_{opt}(N_3^-) = 0.14$$

which is the reverse order of the d transition complexes. The oscillator strength of the Eu(III) azido complex charge-transfer band is approximately 4 times greater than that of the corresponding thiocyanate complex. One possible reason for these differences is the different orientation of the linear NCS^- and N_3^- ions in europium(III) complexes. This feature will be discussed later, because the NMR results showed that Eu-

(17) L. J. Nugent, R. D. Baybarz, J. L. Burnett, and J. L. Ryan, *J. Phys. Chem.*, **77**, 1528 (1973).
(18) C. K. Jørgensen, *Prog. Inorg. Chem.*, **12**, 141 (1970).

Table II. Formation Constants of 4f and 5f Trivalent Aqueous Azido Complexes from f–f Transition Band Intensities

ion	β_1	β_2	ion	β_1	β_2
Nd(III)[a]	1.2	imprecise	Am(III)[c]	10	23
Er(III)[b]	1.2	imprecise	Cm(III)[d]	8	24

[a] Least-squares adjustment of OD at 583.5 nm, as a function of $[N_3^-]$, to eq 3. [b] Least-squares adjustment of OD at 525 nm, as a function of $[N_3^-]$, to eq 3. [c] Least-squares adjustment of OD at 503 nm, as a function of $[N_3^-]$, to eq 3. [d] Least-squares adjustment of OD at 397 nm, as a function of $[N_3^-]$, to eq 3.

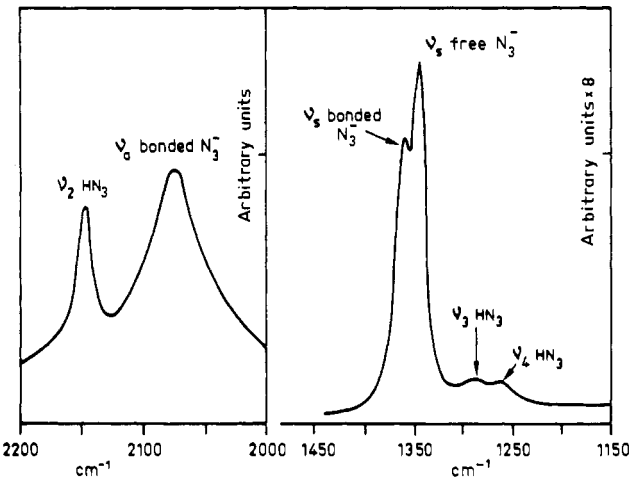

Figure 4. Raman spectrum of NaN_3 in the presence of Ce(III) ($[NaN_3]$ = 1.1 M, [Ce(III)] = 1.3 M, pH 4.4).

$(N_3)^{2+}$ is bent, contrary to the arrangement in $Eu(NCS)^{2+}$, which is linear.

The existence of these charge-transfer bands provides strong evidence for the presence of inner-sphere trivalent lanthanide azide complexes. The formation constant of the Eu(III) 1:1 complex can be easily calculated. The value of 4.0 found was in fair agreement with the results in Table I taken from distribution data, and to within the experimental errors, we can conclude that aqueous lanthanide azide complexes are mostly inner sphere. This view is also supported by the rather important changes in the f–f transition bands, as shown by Figure 3, for complexed Am(III) and Cm(III). Absorption variations can be used to determine the formation constants by invoking eq 5, where ϵ_M represents the mean molecular extinction

$$\epsilon_M = \frac{\sum_{i=0}^{i=n} \epsilon_i \beta_{i1} L^i}{\sum_{i=0}^{i=n} \beta_{i1} L^i} \qquad (5)$$

coefficient at a given wavelength, ϵ_i values are the molecular extinction coefficients for the different species; ϵ_0 refers to the metal hydrated ion, β_{i1} refers to the 1:1 complex, and so on. Formation constants of azide complex from f–f absorption band intensities are given in Table II, showing rather good agreement with values in Table I. Lanthanide azido complex stabilities are not significantly dependent of the atomic number, but the different stabilities for actinide and lanthanide complexes are clearly confirmed. We limited the calculations of the ϵ_i and β_i values by least-squares adjustment to ϵ_1 and β_1 because of the high uncertainties for the high-order ϵ_i, β_i values. However, like the distribution data, spectroscopic data clearly showed the presence of azido complexes containing higher numbers of N_3^- groups, especially the actinides.

The Raman spectra of free N_3^- and bonded N_3^- and HN_3 are shown in Figure 4. The principal features of the bonded N_3^- spectra are as follows. ν_1 symmetric stretching shifts toward higher energy, 1367 cm^{-1} instead of 1347 cm^{-1}. The

Table III. ^{14}N Chemical Shifts (ν) and Transverse Relaxation Time (T_2^{-1}) of Gd(III),[a] Tb(III), and Dy(III) Aquous Azido Complexes

	Gd(III)				
$C_{N_3^-}$, M L^{-1}	$(T_{2M}^{-1})N_{1,3}/p$, 10^{-4} s	$\nu_M/\nu_0 p$, ppm N_2	$N_{1,3}$	Tb(III) $(\nu_M/\nu_0 p)_{N_{1,3}}$, ppm	Dy(III) $(\nu_M/\nu_0 p)_{N_{1,3}}$, ppm
0.836	4.82	442	2615	1912	1375
0.625	3.80	422	1915	1442	1182
0.414	2.32	277	1355	1067	875
0.211	1.55	212	980	692	462
0.102	0.55	115	740	500	345
0.041	0.35	87	365	240	135
0.02	0.15	30	267	87	47

[a] In all these solutions $p = 0.016$ (see text for explanation).

asymmetric ν_3 stretching becomes Raman active and is observed as a broad band at 2075 cm^{-1}, showing that $D_{\infty h}$ symmetry is lost. By monitoring ν_1 intensities with ClO_4^- ν_1 intensities (930 cm^{-1}), we determined β_1 and found a value close to 1.5, in fair agreement with the β_1 values found by other methods. The occurrence of clear bonded N_3^- stretching bands indicates the presence of inner-sphere complexes. However, it is not easy from Raman spectroscopy to determine exactly how N_3^- and trivalent lanthanide are linked. In the absence of polynuclear complexes, this leaves the possibility of configurations like I–III for the 1:1 complex. ^{14}N and ^{15}N nuclear magnetic resonance studies were performed to solve this problem.

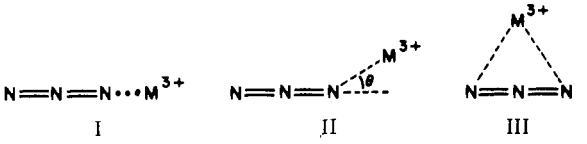

I II III

NMR Investigations

At room temperature, NMR spectra of $Na^{14}N_3$–$H^{14}N_3$ mixtures exhibit only two signals. The addition of small amounts of paramagnetic lanthanides shifts the signal toward higher fields and causes a broadening of the lines without the appearance of new lines. As it is known that HN_3 has the type II conformation with θ angle close to 68°, these spectra are understandable on the basis of: fast exchanges of H^+ and metal and the equivalence of nitrogens 1 and 3. Peak assignment can be carried out easily from the integrated intensities. ^{14}N chemical shifts and line broadening were measured as a function of azide concentration for Gd(III), Tb(III), and Dy(III) solutions. The results are given in Table III. Experimental results from several solutions with different p values ($p = C_{metal}/C_{ligand}$) were corrected by using formulas 6 and 7, valid for fast-exchange conditions, where Δ_{obsd} is an

$$\Delta_{obsd} = \Delta_0(1 - p\bar{q}) + p\bar{q}\Delta_M \quad (6)$$

experimentally observable chemical shift or transverse relaxation time, Δ_0 is the observable value for the pure ligand solution, $\bar{q}$ is the mean number of bonded azides per metal atom, and Δ_M is the observable value for the bonded azide in the metal coordination sphere. When $(C_{ligand})_t >> C_{metal}$, eq 6 becomes

$$\Delta_{obsd} - \Delta_0 = p\bar{q}\Delta_M \quad (7)$$

It may be seen from the values in Table III than lanthanide coordination to azide has a much stronger effect on $N_{1,3}$ nitrogen signals than on those of N_2, indicating a strong screening effect for spin density transfer to N_2. In covalent azides,[19] bonded as shown in model II, similar behavior was

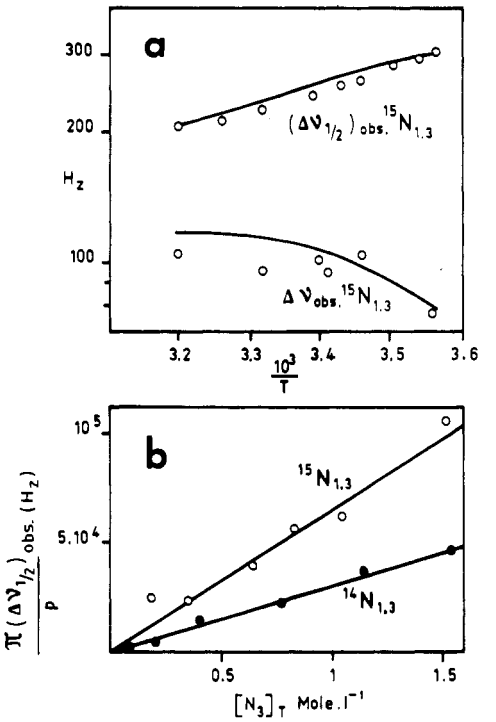

Figure 5. (a) Gd(III) azido complex $^{15}N_{1,3}$ NMR chemical shift ($\Delta\nu$) and line broadening ($(\Delta\nu_{1/2})_{obsd}$) as a function of reciprocal temperature ($p\bar{q} = 10^{-2}$). (b) Comparison of line broadening for $^{14}N_{1,3}$ and $^{15}N_{1,3}$ NMR signals of Gd(III) azido complexes as a function of NaN_3 concentration (pH 5.5).

observed, except that slow exchange served to rank $\Delta_{obsd}(N_1) > \Delta_{obsd}(N_3) >> \Delta_{obsd}(N_2)$.

The temperature dependence of $\Delta\nu$ (^{15}N chemical shift) and $\Delta\nu_{1/2}$ (line width) were examined. The results for a solution 0.87 M in N_3^- and 0.008 M in Gd^{3+} ($p\bar{q} = 10^{-2}$) are plotted in Figure 5a.

As for SCN^- complexes,[3] the shape of these curves indicates that at 300 K the exchange is fast with τ_h (residence time of the ligand), shorter than 10^{-7} s. ^{15}N NMR studies of Gd(III) azido complexes were carried out, and additional proof of fast exchange can be seen in Figure 5b, where $\Delta\nu_{1/2}(^{14}N)/\Delta\nu_{1/2}(^{15}N)$ line width ratios are plotted as a function of N_3^- concentration. The ratio remains constant and equal to 2.07, a value fairly comparable to 1.97, the square of the gyromagnetic ratio of ^{15}N to ^{14}N. $(\gamma_{^{15}N}/\gamma_{^{14}N})^2$. A more extensive demonstration of the validity of these tests was given for the SCN^- gadolinium complexes.[3]

Complex formation constants can be calculated from NMR data by either chemical shifts or line broadening, with use of the equation

$$\bar{q} = \frac{\Delta_{obsd}}{\Delta_M p} = \sum_1^n i\beta_{i1}X^i / \sum_0^n \beta_{i1}X^i \quad (8)$$

where β_{i1} is the formation constant of the MX_i complex and X is the ligand concentration.

Equation 8 implies that the observable variation is independent of the nature of the complexes in which N_3^- groups are engaged. For example, $Gd(N_3)_2^+$ chemical shift and line broadening must be twice those of $Gd(N_3)^{2+}$. In our case, this condition was satisfied for Gd(III) complexes on the basis of the close $\bar{q}$ values determined by using either chemical shifts or line width. The values of $\Delta\nu_{1/2}$ and T_2^{-1} in Table III were introduced into eq 8 to calculate the best set of constants β_{i1} by the least-squares method. The $\bar{q}$ value for $[N_3^-] = 1$ M, taken from the extraction data, was used for the calculations because the Δ_M value was unknown. The NMR β_{i1} complex formation constants are fairly comparable to the β_{i1} values

(19) W. Beck, W. Becker, K. F. Chew, W. Derbyshire, N. Logan, D. M. Revitt, and D. B. Sowerby, *J. Chem. Soc., Dalton Trans.*, 245 (1972).

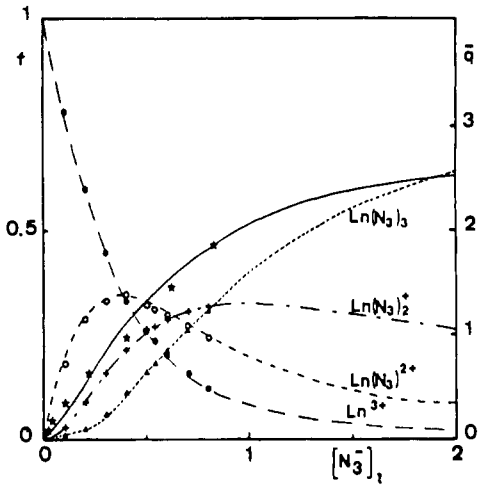

Figure 6. Comparison between azido species distributions calculated with Table I formation constants (curves) and calculated from NMR data (points).

obtained from extraction, as shown in Figure 6, where the Nd(III) species concentration and $\bar{q}$ values are plotted as a function of N_3^- concentration. The solid lines represent the extraction data and the points the NMR results. This good agreement means that, within the N_3^- concentration range investigated, there is no change in the azide coordination mode and that we are still dealing with inner-sphere complexes.

Longitudinal relaxation rates of ^{15}N (T_{1M}^{-1}) were measured to gain some insight into the complex geometry. In extreme narrowing conditions T_{1M}^{-1} and Gd–N internuclear distance are related by eq 9. γ_I and γ_S are respectively the nuclear

$$T_{1M}^{-1} \simeq 6.3(\gamma_I\gamma_S\hbar)^2 r^{-6}\tau_r \quad (9)$$

and electron gyromagnetic ratios, and r is the Gd^{3+}–nucleus distance. τ_r is the complex reorientation correlation time, which was estimated from the relaxation of the water protons, the Gd–H distance (3.1 Å) being taken from ref 20 and eq 9 and 10 being used.

$$T_{1HDO}^{-1} = (T_{1HDO}^{-1})_{obsd}/p\bar{q}_{H_2O} \quad (10)$$

The number of $\bar{q}_{H_2O}$ is the average number of water molecules in the Gd(III) azido complex first coordination sphere. It was estimated by the equation $\bar{q}_{H_2O} = 8 - \bar{q}$, where $\bar{q}$ is the number of azide ions in the complex and 8 the number of inner-sphere water molecules in noncomplexed Gd(III). It was taken from the paper of Steele et al.,[20] and we assumed that in the complex one water molecule is replaced by one N_3^- ion.

We did find $T_{1HDO}^{-1} = 114000\ s^{-1}$ at 300 K, and eq 9 yields $\tau_r = 5.5 \times 10^{-11}$ s.

By measuring $(T_1^{-1})_{N_{1,3}}$ and $(T_1^{-1})_{N_2}$, the geometry of the Gd—N_1=N_2=N_3 moiety can be determined from the equation

$$\frac{r_{N_2}}{r_{N_{1,3}}} = \left(\frac{(T_1)_{N_2}}{(T_1)_{N_{1,3}}}\right)^{1/6} \quad (11)$$

If it is taken into account that

$$(T_1^{-1})_{N_{1,3}} = \tfrac{1}{2}[(T_1^{-1})_{N_1} + (T_1^{-1})_{N_3}] \quad (12)$$

eq 11 becomes

$$\frac{(T_1)_{N_{1,3}}}{(T_1)_{N_2}} = \frac{2r_2^{-6}}{r_1^{-6} + r_3^{-6}} \quad (13)$$

(20) M. L. Steele and D. L. Wertz, *J. Am. Chem. Soc.*, 98, 4424 (1976).

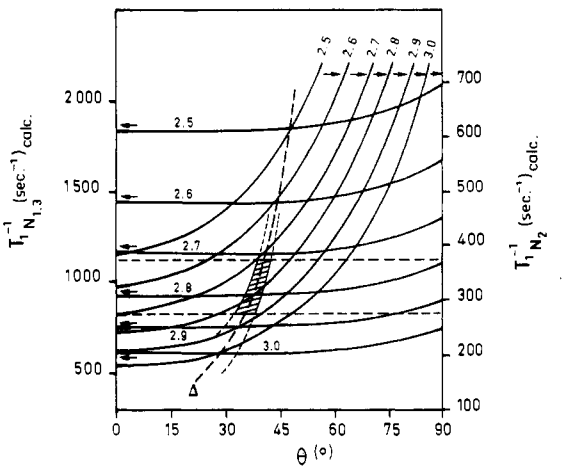

Figure 7. Calculated $(T_1^{-1})_{N_{1,3}}$ and $(T_1^{-1})_{N_2}$ values as a function of θ (see text). The figures indicate the N_1 to Gd distances. The two horizontal dashed lines on either side of the Δ line represent the measured T_1^{-1} values within the limits of experimental uncertainties.

Table IV. S_F Values for Selected Ligands (Am(III)-Eu(III))

ligand	complex	S_F	donor atom electronegativity
F^-	MF^{2+}	−0.084	4.0
$CH_3CO_2^-$	$M(CH_3CO_2)^{2+}$	0.03	3.5
N_3^-	$M(N_3)^{2+}$	0.93	3.0
phen[a]	$M(phen)^{3+}$	0.69	3.0
TPTZ[b]	$M(TPTZ)^{3+}$	0.38	3.0

[a] 1,10-Phenanthroline. [b] 2,4,6-Tri-2-pyridyl-1,3,5-triazine.

Moreover, eq 14 and 15 correlate r_{N_2} and r_{N_3} values to r_{N_1} and the Gd—N=N=N angle (θ).

$$r_{N_2} = [(r_{N_1}\cos\theta + 1.12\ (Å))^2 + (r_{N_1}\sin\theta)^2]^{1/2} \quad (14)$$

$$r_{N_3} = [(r_{N_1}\cos\theta + 2.24\ (Å))^2 + (r_{N_1}\sin\theta)^2]^{1/2} \quad (15)$$

The best values of the r_{N_1} = Gd–N_1 distance and of the binding angle θ were determined as follows: the relaxation rates $(T^{-1})_{N_{1,3}}$ and $(T_1^{-1})_{N_2}$ were calculated from eq 9 and 13–15 as functions of θ for $\tau_r = 5.5 \times 10^{-11}$ s and different values of r_{N_1} ranging from 2.4 to 3.5 Å. In Figure 7, the plots of $(T_1^{-1})_{N_{1,3}}$ and $(T_1^{-1})_{N_2}$ vs. θ are scaled by the experimental factor $(T_1^{-1})_{N_{1,3}}/(T_1^{-1})_{N_2} \simeq 3$. The dashed line Δ represents the locus of intersections of the $(T_1^{-1})_{N_{1,3}}$ and $(T_1^{-1})_{N_2}$ vs. θ curves. It seemed to us realistic, however, to replace in our calculation the Δ curve by a zone taking into account the experimental uncertainties, of the order of ±5%, on the ^{15}N relaxation rates as well as on the values of τ_r and $\bar{q}$. The intercept of the experimental relaxation rates of $^{15}N_{1,3}$ and $^{15}N_2$ with this zone delineates the hatched area shown in Figure 7, where the most probable values of r_{N_1} and θ are expected to be found. They correspond to $r_{N_1} = 2.78 \pm 0.06$ Å and $\theta = 38 \pm 6°$.

Conclusion

Azides form inner-sphere aqueous complexes with trivalent actinide and lanthanide. The 5f azido complexes are the more stable, probably because higher covalent interactions take place within the 5f shell.

In order to compare several ligands with regard to their selectivity toward a trivalent actinide–lanthanide pair, we calculated a selection factor S_F defined by eq 16, where the

$$S_F = 2(\Delta G_{Am(III)} - \Delta G_{Eu(III)})/\Delta G_{Am(III)} - \Delta_{Eu(III)} \quad (16)$$

ΔG values are the free energy changes for homologous complexes. Selected S_F values are given in Table IV. It may be observed that the highest S_F value is found for the pair Am-

$(N_3)^{2+}$-$Eu(N_3)^{2+}$. All the pure nitrogen ligands are in the group of high S_F values. Similarly, covalent interactions are the cause of these high selection factors, since the ionic radii of Am(III) and Eu(III) (1.09 and 1.06 Å) suggest that, for pure ionic bonds, the Eu(III) complexes will be the more stable. This trend is observed in the fluoride complexes.

However, it is unlikely that the type II geometry found for $Gd(N_3)^{2+}$ arises from the presence of a covalent bond with a sp^2-hybridized nitrogen strongly linked to the metal, as in trivalent d transition azido complexes, for which β_{11} values are several orders of magnitude higher than the β_{11} of the lanthanide complexes. The N_3^- position probably results from the action of antagonistic forces. Azide negative charge density is equally shared between N_1 and N_3 nitrogens,[21] and N_3^- ions are ionically attracted by the metal and the nearest water molecules. The observed position is most probably the resultant of these two kinds of interactions.

The investigation of hexa- and tetravalent azido complexes of actinides supports these assumptions.[22] Configuration III was found in U(VI) complexes. The linearity of $M(NCS)^{2+}$ lanthanide species could also be understood from the predominantly ionic interactions, because the negative charge densities carried by sulfur and nitrogen[21] are smaller than those of N_3^- terminal nitrogen, as shown in IV and V, and the linear configuration is favored.

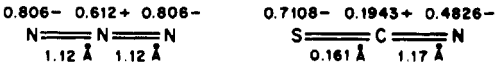

IV V

The spin density transferred from Gd(III) to N_3^- is slightly higher to the spin transferred[3] from Gd(III) to NCS^- or to the solvation water molecules[23] but is one order of magnitude lower than the spin density transferred from Co(II) to NCS^-.[24]

Acknowledgment. We are indebted to Prof. R. Guillaumont, who welcomed C. Cuillerdier into his laboratory to start the solvent-extraction investigations.

(21) S. M. Nelson, *MTP Int. Rev. Sci.: Inorg. Chem., Ser. One*, **5**, 211 (1972).

(22) C. Musikas et al., to be submitted for publication in *Inorg. Chem.*
(23) J. Reuben and D. Fiat, *J. Chem. Phys.*, **51**, 4909 (1969).
(24) A. H. Zeltmann and L. O. Morgan, *Inorg. Chem.*, **9**, 2522 (1970).

Contribution from the Institut für Physikalische und Theoretische Chemie and Physikalisches Institut, Abt. II, University of Erlangen-Nürnberg, D-8520 Erlangen, West Germany, and the School of Chemistry, University of New South Wales, Kensington, NSW 2033, Australia

Nature of the Continuous High-Spin ($^5T_2$) ⇌ Low-Spin ($^1A_1$) Transition in Bis[2-((4-methyl-2-pyridyl)amino)-4-(2-pyridyl)thiazole]iron(II) Diperchlorate Dihydrate and Bis(tetrafluoroborate) Dihydrate: Mössbauer Effect and X-ray Diffraction Study

E. KÖNIG,*[1a] G. RITTER,[1b] S. K. KULSHRESHTHA,[1a,c] and H. A. GOODWIN[2]

Received October 7, 1982

The gradual high-spin ($S = 2$, $^5T_2$) ⇌ low-spin ($S = 0$, $^1A_1$) transformations in solid $[Fe(4\text{-paptH})_2](ClO_4)_2 \cdot 2H_2O$ and $[Fe(4\text{-paptH})_2](BF_4)_2 \cdot 2H_2O$ (4-paptH = 2-((4-methyl-2-pyridyl)amino)-4-(2-pyridyl)thiazole) have been studied by variable-temperature ^{57}Fe Mössbauer effect and X-ray diffraction. For the complex perchlorate, the ground states involved are characterized, at the transition temperature $T_c \approx 185$ K, by the quadrupole splitting $\Delta E_Q(^5T_2) = 2.40$ mm s^{-1}, $\Delta E_Q(^1A_1) = 1.31$ mm s^{-1} and the isomer shift $\delta^{IS}(^5T_2) = +1.05$ mm s^{-1}, $\delta^{IS}(^1A_1) = +0.42$ mm s^{-1}. For the complex tetrafluoroborate, the corresponding values at the transition temperature $T_c \approx 220$ K are $\Delta E_Q(^5T_2) = 2.40$ mm s^{-1}, $\Delta E_Q(^1A_1) = 1.32$ mm s^{-1} and $\delta^{IS}(^5T_2) = +1.01$ mm s^{-1}, $\delta^{IS}(^1A_1) = +0.39$ mm s^{-1}. The observed nonlinear temperature dependence of $-\ln(\sum t_i)$, where t_i is the effective thickness ($i = {}^5T_2, {}^1A_1$), is consistent with different Debye-Waller factors, $-\ln f_{^5T_2}$ and $-\ln f_{^1A_1}$. The same conclusion is indicated by the observation of different temperature factors for the isomer shift. The lattice spacings derived from X-ray diffraction show a continuous variation with temperature which parallels that of the $^5T_2$ fraction, $n_{^5T_2}$. The results are interpreted in terms of the formation of a solid solution of the two spin isomers within the one lattice. The continuous character of the transition is consistent with the assumption of weak cooperative interaction between the individual complexes and a wide distribution of the nuclei of the minority constituent.

Introduction

The discontinuous type high-spin ($^5T_2$) ⇌ low-spin ($^1A_1$) transitions in solid compounds of iron(II) now seem to be reasonably well understood. Such transitions arise for compounds with a strong cooperative interaction between the individual complexes. In the transition region, pronounced domain formation by both minority and majority phases is encountered, and thus individual X-ray diffraction patterns for the two phases are observed. Due to the interaction, a crystallographic phase change is, in general, involved. Hysteresis effects, if present, are a consequence of the domain formation. To date, consistent results have been derived from the temperature dependence of X-ray diffraction and Mössbauer effect data for a number of systems, i.e. for $[Fe(phy)_2](ClO_4)_2$ (where phy = 1,10-phenanthroline-2-carbaldehyde phenylhydrazone),[3] $[Fe(bt)_2(NCS)_2]$ (where bt = 2,2′-bi-2-thiazoline),[4] $[Fe(4,7\text{-}(CH_3)_2phen)_2(NCS)_2]$ (where 4,7-$(CH_3)_2$phen = 4,7-dimethyl-1,10-phenanthroline),[5] and $[Fe(bi)_3](ClO_4)_2$ (where bi = 2,2′-bi-2-imidazoline).[6] It thus seems that the conclusions are of general applicability to spin transitions of the discontinuous type.

(1) (a) Institut für Physikalische und Theoretische Chemie, University of Erlangen-Nürnberg. (b) Physikalisches Institut, Abt. II, University of Erlangen-Nürnberg. (c) On leave of absence from the Chemistry Division, Bhabha Atomic Research Centre, Bombay, India.
(2) University of New South Wales.

(3) König, E.; Ritter, G.; Irler, W.; Goodwin, H. A. *J. Am. Chem. Soc.* **1980**, *102*, 4681.
(4) König, E.; Ritter, G.; Irler, W.; Nelson, S. M. *Inorg. Chim. Acta* **1979**, *37*, 169.
(5) König, E.; Ritter, G.; Irler, W. *Chem. Phys. Lett.* **1979**, *66*, 336.
(6) König, E.; Ritter, G.; Kulshreshtha, S. K.; Nelson, S. M. *Inorg. Chem.* **1982**, *21*, 3022.

0020-1669/83/1322-2518$01.50/0